Estuaries and Coasts (2013) 36:728–736
DOI 10.1007/s12237-013-9591-6

Cell Size-Dependent Effects of Solar UV Radiation on Primary Production in Coastal Waters of the South China Sea

Gang Li · Kunshan Gao

Received: 13 September 2012 / Revised: 24 December 2012 / Accepted: 14 January 2013 / Published online: 1 March 2013

Abstract In order to examine the effects of solar ultraviolet radiation (UVR, 280–400 nm) on photosynthesis of differently cell-sized phytoplankton, natural phytoplankton assemblages from the coastal waters of the South China Sea were separated into three groups (>20, 5–20, and <5 μm) and exposed to four different solar UV spectral regimes, i.e., 280–700 nm (PAR+UVR), 400–700 nm (PAR), 280–400 nm (UV-A+B), and 315–400 nm (UV-A). In situ carbon fixation measurements revealed that microplankton (>20 μm) efficiently utilized UV-A for photosynthetic carbon fixation, with assimilation number of up to 1.01 μg C (μg chl *a*)$^{-1}$h^{-1} under 21.4 Wm^{-2} UV-A alone (about half of noontime irradiance at the surface), about 40 % higher than nanoplankton (5–20 μm). UV-B (280–315 nm) of 0.95 Wm^{-2} reduced the carbon fixation by approximately 20 and 57 % in microplankton and nanoplankton assemblages, respectively. In contrast, smaller picoplankton (<5 μm) was unable to utilize UV-A for the photosynthetic carbon fixation. In addition, only micro-sized assemblages demonstrated the UV enhancement on their primary productivity in the presence of PAR, by about 8 % under moderate intensities of solar radiation.

Keywords Cell size · UVR · Carbon fixation · Phytoplankton · South China Sea

G. Li · K. Gao (✉)
State Key Laboratory of Marine Environmental Science, Xiamen University, Xiamen, Fujian 361005, China
e-mail: ksgao@xmu.edu.cn

G. Li
Key Laboratory of Marine Bio-resources Sustainable Utilization, South China Sea Institute of Oceanology, Chinese Academy of Sciences, Guangzhou, Guangdong 510301, China

Introduction

Due to the stratospheric ozone depletion and climate-related changes, marine phytoplankton are subject to increasing UV-B (280–315 nm) irradiance and fluctuations of ultraviolet radiation (UVR, 280–400 nm) during daily or seasonal cycles (Häder et al. 2007). Solar UVR is known to damage DNA, protein molecules, and pigments (Buma et al. 2003; Roy et al. 2006), reduce photosynthesis (Gao et al. 2009; Li et al. 2011) and nutrient uptakes (Hogue et al. 2005), and even lead to cell death (Agustí and Llabrés 2007). Additionally, UVR can cause changes in community structures (Davidson et al. 1996) and ultimately influence the marine food chains (Häder et al. 2007; Häder 2011). However, moderate intensities of UV-A (315–400 nm) can also aid in photorepairing UV-B-damaged DNA (Karentz et al. 1991; Buma et al. 2003). UV-A-driven photosynthesis in micro- as well as macro-algae has also been reported under the reduced or fluctuating solar radiation (Helbling et al. 2003; Mengelt and Prézelin 2005; Gao et al. 2007a; Xu and Gao 2010).

Cell size of phytoplankton crucially determines the efficiency of element or energy transfer and, thus, the production of higher trophic levels in marine food webs (Raven 1998; Finkel et al. 2010; Mei et al. 2011). Light absorption (Sigee 2005; Fujiki and Taguchi 2002), photosynthesis (Raven and Kübler 2002; Li et al. 2011), and tolerance to UVR (Laurion and Vincent 1998; Häder 2011) are also known to differ among differently cell-sized phytoplankton. Pigment-specific light absorption increases with decreasing cell size (Fujiki and Taguchi 2002), leading to a higher light use efficiency as well as UV exposure per unit pigment or per cell volume (Jeffrey et al. 1996); therefore, smaller cells are usually more vulnerable to UV than their larger counterparts (Garcia-Pichel 1994; Laurion and Vincent 1998). In general, smaller phytoplankton cells

dominate the pelagic water (Li 2002; Finkel et al. 2010), whereas larger cells dominate the coastal water wherein the cell assemblages are more resistant to solar UVR (Li et al. 2011). However, little has been documented on the size-dependent effects of UV on photosynthetic carbon fixation of the phytoplankton assemblages, as well as the effective UV wavebands.

Cell size of phytoplankton tends to vary greatly from nutrient-rich coasts to oligotrophic oceans (Raven 1998; Li 2002; Finkel et al. 2010) and from well-mixed winter to severely stratified summer conditions [i.e., larger cells are abundant in the former, while smaller ones are plentiful in the latter (Chen 2005; Wu et al. 2010)]. Along with the different wavebands of UV that attenuate differentially down the water column, phytoplankton cells at different depths and of different sizes can be affected to a different extent. Here, we studied the cell size-dependent photosynthetic carbon fixation of natural assemblages from the coastal waters of the South China Sea and looked into the roles of UV on regulating the marine primary productivity.

Materials and Methods

Sample Collection Surface seawater samples (20 cm) containing phytoplankton assemblages were collected from the coastal waters of the South China Sea at Nan'ao (23°29′ N, 117°06′ E; 10 m deep and 500 m offshore) and Xisha coral reefs (16°51′ N, 112°20′ E; 20 m deep and 300 m offshore) near Yongxing Island (Fig. 1). The study was carried out during the periods of August 2006 and March to July 2007.

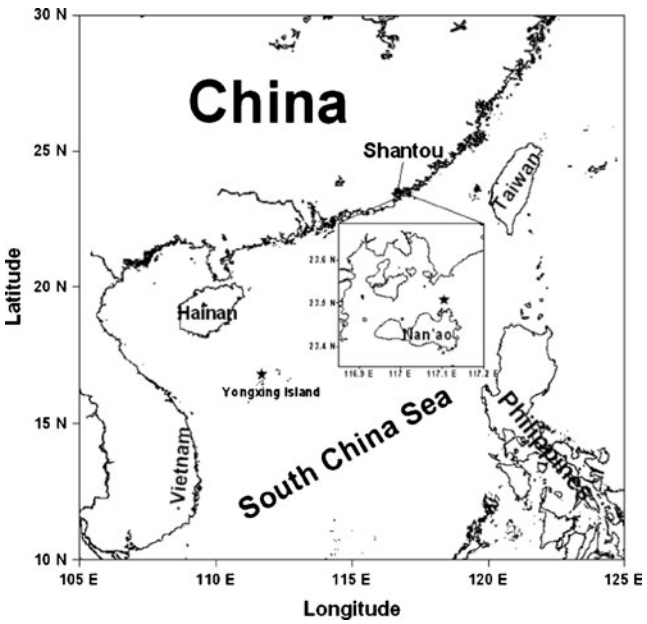

Fig. 1 Sampling sites in Nan'ao and Xisha waters of the South China Sea

The samples were collected in the morning (around 0830 hours) with an acid-cleaned (1 N HCl) polycarbonate container. The temperature and salinity were measured with a conductivity–temperature–depth equipment (YSI 600XL, Yellow Springs Instruments, USA). Determinations of photosynthetic carbon fixation and other related analyses (described below) were done or initiated within 15 min of the sampling.

Irradiance Measurements Incident solar irradiance was continuously monitored with a broadband solar radiometer (ELDONET, Real Time Computer Inc., Germany) that measured every second the solar irradiance of UV-B (280–315 nm), UV-A (315–400 nm), and PAR (400–700 nm), and recorded the means over each minute (Häder et al. 1998). During the study period, the equipment was set on the roof of a building, about 200 m off the sampling site in both Nan'ao and Xisha. The light penetration in Xisha water were measured with a diving radiometer (ELDONET, Real Time Computers, Inc.) with the same channels as mentioned above as well as temperature and depth sensors. The equipments are authenticated accurately (certificate no. 2006/BB14/1) with less than 0.5 % error and calibrated regularly using a double monochromator spectroradiometer (HR4000, Oceanic Optics Inc., USA) and a certified calibration lamp (DH 2000, Oceanic Optics Inc., USA).

Size Fractionation To obtain three cell size fractions of phytoplankton assemblages, prefiltered seawater (180-μm pore size; to remove large zooplankton) was sequentially filtered through a 20- and 5-μm pore size Nitex® mesh; the cells that reposed on the meshes were gently washed off using filtered (Whatman GF/F filter) seawater and diluted to their natural abundance level. The diluted samples (>20- and 5–20-μm fractions) and filtrates (<5-μm fraction) were used for experiments. For simplicity, phytoplankton cells with effective diameter >20 μm were classified as microplankton, 5–20 μm as nanoplankton, and <5 μm as picoplankton hereafter.

Experimental Design Subsequent to the collections, the seawater samples were exposed to different solar irradiation treatments to determine the photosynthesis vs. UV relationship (P vs. U curves), photosynthesis vs. PAR relationship (P vs. E curves), and UV spectral irradiance effects on carbon fixation as follows (Table 1).

The P vs. U curves of the three size-based phytoplankton assemblages (>20, 5–20, and <5 μm) were established in Nan'ao coastal water under two irradiation treatments, i.e., (a) samples exposed to UV-A+B (UVR, 280–400 nm) in quartz tubes covered with Schott UG-11 filter (50 % cutoff at 280 and 375 nm, and transmit between them), and (b) samples exposed solely to UV-A (320–400 nm) in quartz tubes covered with UG-11+Folex 320 filter (50 % cutoff at

Table 1 Experimental information and solar radiation penetration depths (1 % of surface irradiance) of the sampling sites in Nan'ao and Xisha waters

	Experiment	Date	Size fraction	Light penetration		
				PAR (m)	UV-A (m)	UV-B (m)
Nan'ao	P–U curve	Jun 27 and 28, Jul 5, 2007	<5, 5–20, and >20 μm	6–8[a]	3–3.5[a]	1.7–2.3[a]
	P–E curve	Jun 24 and 26, 2007	<20 and, >20 μm			
	UV spectra	Aug 2 and 6, 2006; Jun 23, 2007	Total cell assembly			
Xisha	P–U curve	March 28 and 30, 2007	Total cell assembly	22	12	8.4

P–U curve, P–E curve, and UV spectra represent the photosynthesis vs. UV relationship, photosynthesis vs. PAR relationship, and effects of UV spectral irradiance on carbon fixation, respectively. The light penetration in Xisha water was measured on March 24, 2007

[a] Light penetration in Nan'ao water based on Gao et al. 2007b, measured in summer of 2005

320 nm). However, in the case of Xisha samples, total assemblages were used since about 90 % of the cells had a diameter <5 μm (Table 2). All the incubations were carried out in triplicates. The tubes containing phytoplankton samples were placed beneath a UG-11 filter to cut off PAR; furthermore, in order to obtain different UV intensities, zero (none) to five layers of neutral density net were employed to vary UVR from 54 to 3 % of its incident surface level (Gao et al. 2007a). Two incubation days (March 28 and 30, 2007) were used in Xisha water with three light intensities for each day; and three incubation days (June 27, 28, and July 5, 2007) were used in Nan'ao water with three cell fractions under two light intensities for each day.

The P vs. E curves of two cell-sized assemblages (>20 and <20 μm) in Nan'ao coastal water were obtained in the presence and absence of UVR as follows: (a) samples exposed to PAR+UVR (cells receiving irradiances above 280 nm) in uncovered quartz tubes; and (b) samples exposed to PAR alone (cells receiving irradiances above 395 nm) in quartz tubes wrapped with Ultraphan 395 filter (50 % cutoff at 395 nm). Nine intensities (triplicate for each) of solar radiation from 100 to <2 % of surface irradiance were achieved by covering the samples with zero to seven layers of neutral density screens (Li et al. 2009). For the P–E curves, two incubation days (June 24 and 26, 2007) were used with two cell size fractions under four or five light intensities for each day.

To study the effects of UV spectral irradiance on photosynthetic carbon fixation, total phytoplankton assemblages in quartz tubes were placed in an opaque plastic box (in triplicates) that was sealed with a UG-11 filter on the top, so that the cells were exposed either to full solar UV spectrum (uncovered tubes) or different UV spectral irradiance by covering the UG-11 with WG295, WG305, WG320, or WG360 nm Schott cutoff filters. For the radiation treatments with PAR plus different UV wavebands, the UG-11 filter was removed. This set of experiment was carried out on August 2 and 6 2006 and June 23 2007, respectively. Xu and Gao (2010) have presented the transmission spectra of Folex 320 (Montagefolie, no. 10155099, Folex, Dreieich, Germany), Ultraphan 395 (UV Opak, Digefra, Munich, Germany), and UG-11 filters (Schott, Mainz, Germany), while those of the WG filters can be found in Villafañe et al. (2003). The UG-11 filter cuts off 100 % PAR and transmits 53.7 % UV-A and 63.8 % UV-B, whereas Folex 320 foil transmits 70.5 % UV-A (Gao et al. 2007a). There was about 5-nm difference between the measured (315–400 nm) and exposed UV-A (320–400 nm) waveband, so the cells received about 2 % less UV-A irradiance as compared to the measured irradiance.

Table 2 Physical and biological features (mean±SD, n=3–8) in surface seawater of Nan'ao and Xisha: mean solar irradiance (in Watt per square meter) of PAR, UV-A, and UV-B during the ^{14}C-labeled incubations, surface seawater temperature (SST, in degrees Celsius), and salinity (SSS), chl *a* concentration (in microgram per liter), and proportion (in percentage) to total chl *a* of the three cell-sized fractions for the periods of June 24 to August 8, 2006 and June 23 to 26 of 2007 in Nan'ao water and March 23 to 31 of 2007 in Xisha water

	PAR	UV-A	UV-B	SST	SSS	chl *a*	>20 μm	5–20 μm	<5 μm
Nan'ao	313±74	47.7±10	2.1±0.4	26.2±1.5	27.7±3.8	6.23±3.0	42±12.6	22.3±6.7	35.8±4.1
Xisha	360±10	55.6±1.7	2.6±0.1	29.1±1.4	33.9±0.1	0.53±0.18	–	–	88.4±5.4

Photosynthetic Carbon Fixation The pretreated water samples were dispensed into 20- or 50-mL quartz tubes and inoculated with 100 μL of 5 μCi (0.185 MBq) $NaH^{14}CO_3$ (ICN Radiochemicals), as 9.25- or 3.7-kBqpermL samples; the tubes were then incubated for 6 h (0930–1530 hours) in a water tank supplied with a continuous flow of surface seawater to maintain the temperature at 26–28 °C in Nan'ao or at 28–30 °C in Xisha water (similar to surface seawater temperature (SST)). Duplicate tubes wrapped in aluminum foil were used as dark samples. After the incubation, each sample was filtered onto a Whatman GF/F glass fiber filter (25 mm), placed into a 20-mL scintillation vial, exposed to HCl fumes overnight, dried (55 °C) to expel non-fixed ^{14}C, and digested in 3-mL scintillating cocktail (UltimaGold, Perkin Elmer®); the incorporated ^{14}C was measured using a liquid scintillation counter (Beckman Coulter, LS 6500, USA). The photosynthetic rate was calculated according to Holm-Hansen and Helbling (1995).

Chlorophyll a Measurement Chlorophyll *a* (chl *a*) concentration was measured by filtering 300–500 mL (Nan'ao) or 1.5 L (Xisha) of prefiltered (180-μm pore size) seawater onto a Whatman GF/F glass fiber filter (25 mm), extracting with 5-mL absolute methanol in the dark for 3 h at room temperature, and then being scanned with a spectrophotometer (UV 2501-PC, Shimadzu, Japan) to obtain the optical density between 280- and 750-nm wavelengths. The chl *a* content was estimated based on the equation of Porra (2002). In order to determine the nano- or picoplankton fractions, a sub-sample was prefiltered through a 20- or 5-μm pore size Nitex® mesh, and chl *a* was determined as described above; estimations on chl *a* of each cell size fractions were calculated by subtractions. Likewise, 300–500 mL of diluted samples mentioned above was also filtered to determine chl *a* content, as compared to the subtracted values.

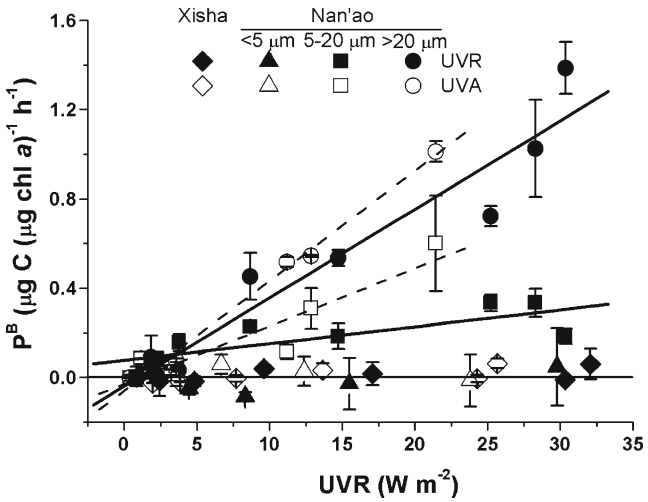

Fig. 2 Photosynthetic carbon fixation rates (in microgram of C per microgram of chl *a* per hour) of differently cell-sized fractions (<5, 5–20, and >20 μm) of phytoplankton assemblages as a function of solar UVR (280–400 nm) or UV-A (315–400 nm) in Watt per square meter during March 28 and 30 in Xisha and June 27, 28, and July 5, 2006 in Nan'ao coastal waters. R^2 values of P vs. U curves (<5 and 5–20 μm) ranged from 0.64 to 0.98 (n=8); the *vertical bars* represent standard deviations (n=3)

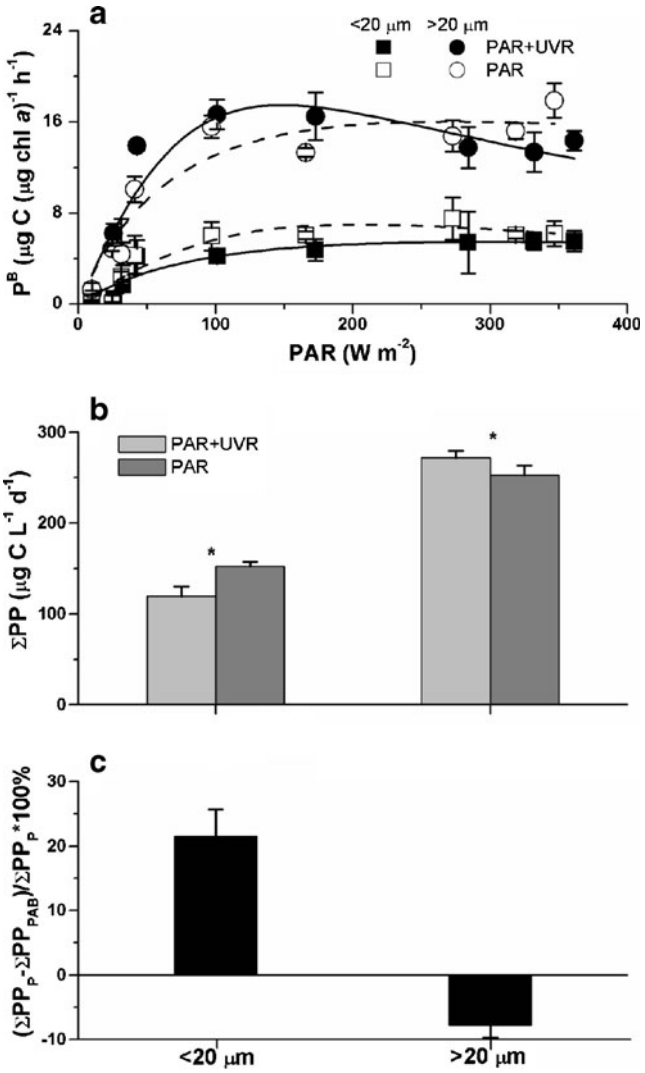

Fig. 3 **a** Photosynthetic rates (in microgram of C per microgram of chl *a* per hour) as a function of PAR irradiance (in Watt per square meter) in microplankton (>20 μm) and pico- and nanoplankton (<20 μm) assemblages from the Nan'ao coastal water on June 24 and 26, 2007 under PAR (280–700 nm) and PAR+UVR (400–700 nm). **b** Daily carbon fixation (in microgram of C per liter per day) of microplankton and pico- and nanoplankton assemblages exposed to two irradiance treatments. **c** Inhibition (in percentage) of UVR on the carbon fixation of microplankton and pico- and nanoplankton cell assemblies. R^2 values of P vs. E curves ranged from 0.72 to 0.86 (n=9); the *vertical bars* represent the standard deviations (n=3), and the *asterisk* indicates significant difference (p<0.05)

Data Analyses P vs. E curves were obtained using the model of Eilers and Peeters (1988) and fitting the data by iteration: $P^B=E/(aE^2+bE+c)$; where, P^B is the photosynthetic rate (in microgram of C per microgram of chl *a* per hour); E is the irradiance (in Watt per square meter); and a, b, and c are the adjustment parameters. Since the Ultraphan 395 filter blocks 4 % of PAR under seawater (Gao et al. 2007a), the establishments of P vs. E (PAR) relationship were performed after calibrating the PAR by multiplying 0.96.

Daily photosynthetic production of microplankton and pico- and nanoplankton cell assemblages was estimated by integrating the carbon fixation rate at different light intensities over the daytime (Behrenfeld and Falkowski 1997): $\sum PP = \int_{t=sunrise}^{sunset} PAR(t)/(a\times\ PAR^2(t) + b \times PAR(t) + c). \times [chl\ a]$; where ∑PP represents the daily carbon fixation (in microgram of C per liter per day); a, b, and c are the adjustment parameters described above; and [chl *a*] is the chl *a* concentration (in microgram per liter).

One-way ANOVA or paired *t* test was used to determine the significant differences between the different irradiation treatments with $p<0.05$; the correlation between the carbon fixation rate and UV intensities was established using a linear regression.

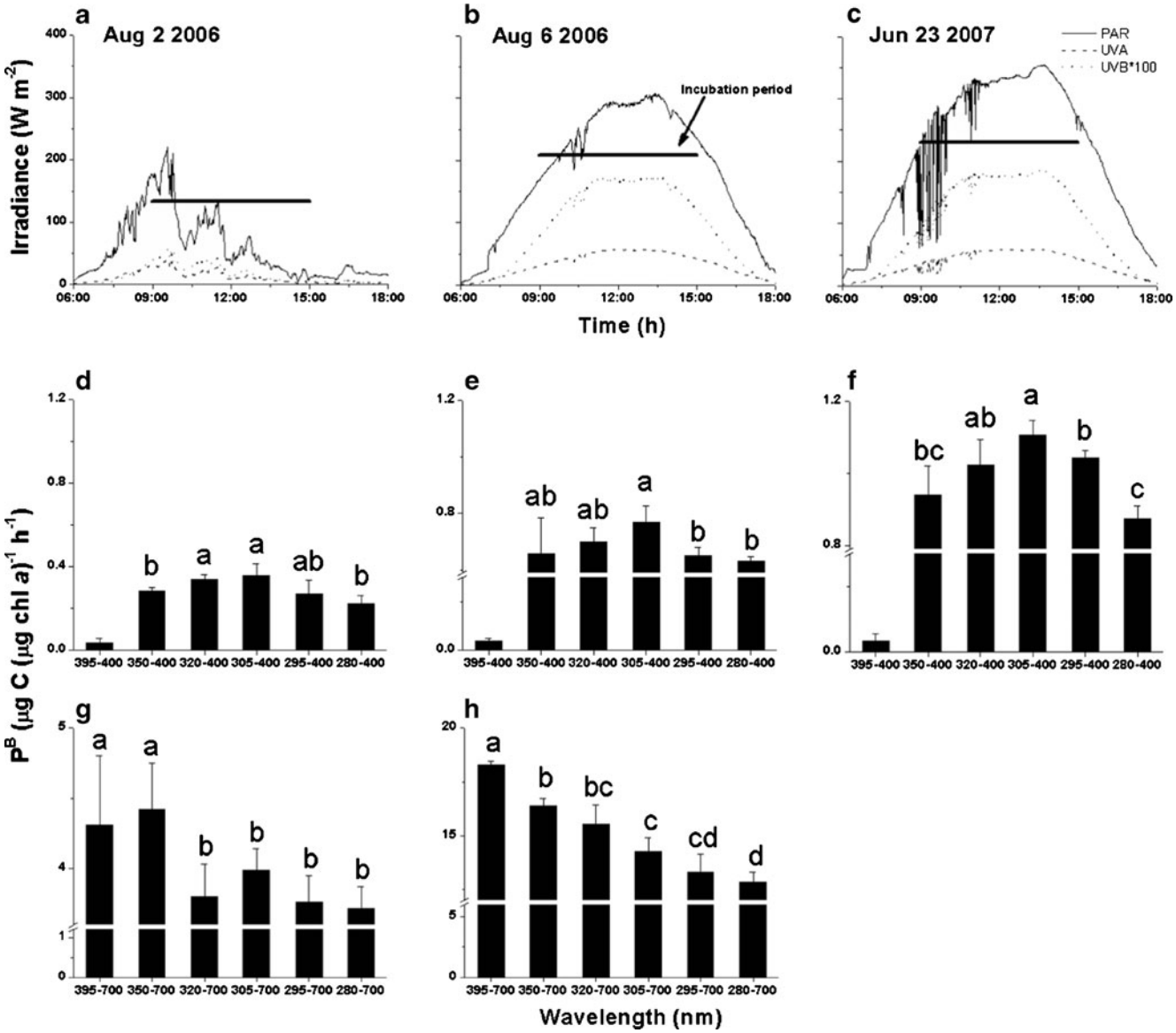

Fig. 4 Incident solar irradiance (in Watt per square meter) of PAR (400–700 nm), UV-A (315–400 nm), and UV-B (280–315 nm) at **a** August 6 and **b** August 8, 2006 and **c** June 23, 2007, when the photosynthetic carbon fixation rate (in microgram of C per microgram of chl *a* per hour) of phytoplankton assemblages were measured under different radiation treatments to distinguish the functional roles of different UV wavebands in the presence (**d**, **e**, **f**) or absence (**g**, **h**) of PAR. The *bold horizontal lines* indicate the incubation periods; the *vertical bars* represent the standard deviations for triplicate incubations; and the *letters* indicate significant difference ($p<0.05$)

Results

Table 2 details the solar irradiance (PAR, UV-A, and UV-B), surface seawater temperature (SST) and salinity (SSS) for the study period, along with phytoplankton biomass (chl *a*) and cell size structure in Nan'ao and Xisha coastal waters. Nan'ao water had relatively lower levels of SST and SSS as compared to Xisha water; while Nan'ao samples demonstrated 12-fold higher chl *a* concentration (6.23±3.0 $\mu g L^{-1}$) as compared to Xisha samples (0.53±0.18 $\mu g L^{-1}$). On the other hand, picophytoplankton contributed to 35.8±4.1 % of total chl *a* in Nan'ao samples, while that of Xisha samples contributed to 88.4±5.4 % (Table 2). Based on the high standard deviations obtained here, it appeared that the physicochemical and biological parameters fluctuated more in Nan'ao than Xisha water (Table 2).

When we exposed samples to UV alone (i.e., when PAR was filtered out), characteristics of P vs. U relationship varied markedly among the three cell-sized assemblages (Fig. 2). Significant photosynthetic carbon fixation occurred when microplankton (>20 μm) or nanoplankton (5–20 μm) cells were exposed to UV, but no noteworthy UV-driven photosynthesis was detected in smaller cells (<5 μm) (Fig. 2). The photosynthetic rate of microplankton assemblages was proportional with increasing UV intensity, i.e., a remarkable increase in photosynthetic rate was found with increasing UV-A intensity, that reached 1.01 μg C(μg chl *a*)$^{-1}h^{-1}$ at 21.4 $W m^{-2}$ (about half of noontime irradiance at the surface); similar results were obtained for nanoplankton cells with the value of 0.60 μg C(μg chl *a*)$^{-1}h^{-1}$ at the same UV intensity (Fig. 2). The apparent photosynthetic efficiency (the initial slope of carbon fixation vs. UV intensity) solely under UV-A was approximately 4.94×10^{-2} and 2.60×10^{-2} μg C(μg chl *a*)$^{-1}h^{-1}$(μmol$m^{-2}s^{-1}$)$^{-1}$ in microplankton and nanoplankton cell assemblies, respectively. Addition of UV-B significantly reduced the photosynthetic efficiency by 20 and 71 % in microplankton and nanoplankton assemblages, respectively. At 10 $W m^{-2}$ of UV irradiance, phytoplankton showed an observed size-dependent variation ($p<0.05$) in carbon fixation abilities when exposed to UV-A+B or UV-A alone. UV-B-induced inhibition on the UV-A-driven carbon fixation reached about 20 % in microplankton cells and 57 % in nanoplankton cells at the highest irradiance (Fig. 2).

The photosynthesis vs. PAR irradiance (P vs. E) relationships of microplankton (>20 μm) and pico- and nanoplankton (<20 μm) assemblages also differed greatly with or without solar UVR (Fig. 3a). Exposure to high intensities of sunlight (PAR >200 $W m^{-2}$) caused greater photoinhibition to microplankton than pico- and nanoplankton cells; this effect was more pronounced in the samples exposed to PAR+UVR (Fig. 3a). At low PAR intensities (i.e., <200 $W m^{-2}$), however, microplankton cell assemblies exposed to PAR+UVR demonstrated higher carbon fixation rates as compared to PAR treatment, reflecting a contribution by UV-driven photosynthesis. However, this phenomenon was not obvious in pico- and nanoplankton cell assemblies (Fig. 3a). Finally, the daily carbon fixation (PAR) of microplankton or pico- and nanoplankton assemblies were about 272 and 120 μg $CL^{-1}d^{-1}$, respectively (Fig. 3b), and the UV exposure increased the daily productivity of microplankton cells by 7.8 % but reduced by 21 % in pico- and nanoplankton cells (Fig. 3c).

Notable differences in the effects of UV spectral irradiance also occurred in the absence and presence of PAR radiation (Fig. 4). Under PAR-free conditions, the samples exposed to 280–400-nm UV demonstrated significant photosynthetic carbon fixation (Fig. 4d–f), with reductions by 14 and 22 % under 280–295- or 295–305-nm UV irradiance, respectively. Compared to total UV bands (280–400 nm), exposures to 305–320- or 320–350-nm irradiance led to 9.1 and 14 % increase in the photosynthetic carbon fixation, respectively (Fig. 5a), implying that the 305–320-nm UV wavebands contribute also to the carbon fixation. In the presence of PAR (Fig. 4g, h), however, deleterious effects of all UV irradiance, i.e., 280–295, 295–305, 305–320, 320–350, and 350–400 nm can be visualized in terms of the inhibition (Fig. 5b).

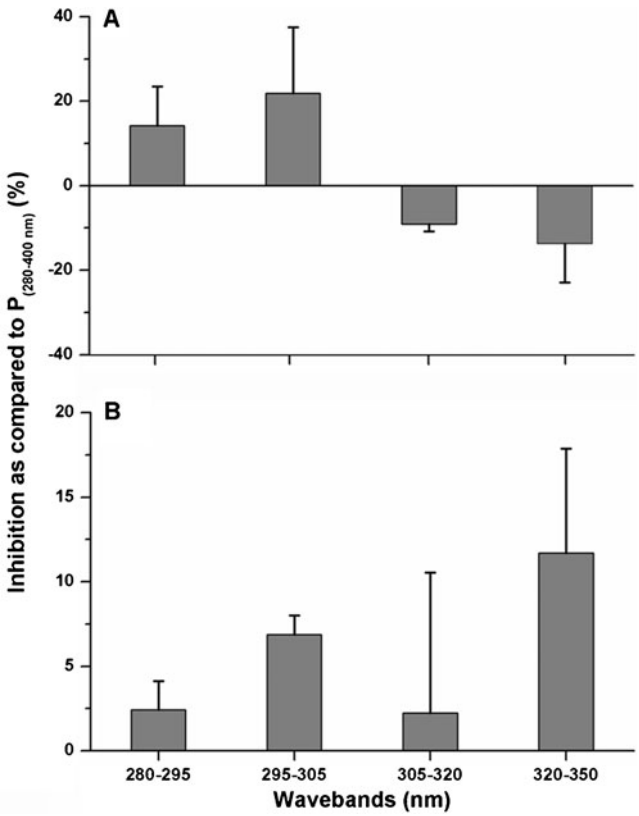

Fig. 5 Inhibition of various UV spectral irradiance on the carbon fixation rate of phytoplankton assemblages. **a** Inhibition (in percentage) as compared to the treatment of 280–400-nm UV irradiance in the absence of PAR. **b** Inhibition (in percentage) as compared to the treatment of 280–700-nm solar irradiance in the presence of PAR

Discussion

Larger phytoplankton cells are known to have slower growth rates as compared to smaller ones due to their slower biomass-normalized metabolic rates, higher nutrient/energy requirements, and faster sinking rates (Raven 1998; Raven and Kübler 2002; Mei et al. 2011). However, this study reveals a new perspective to this theory that larger cells (>20 μm) can benefit from UV radiation since they can use most of UV spectral energy for photosynthesis, while smaller ones (<5 μm) cannot use this energy when PAR is limiting. Previously, UV-A has been indicated to drive photosynthesis of coastal phytoplankton assemblages (Gao et al. 2007a); this study indicates that longer wavebands of UV-B (305–315 nm) might also be used for photosynthesis.

Size-dependent responses of phytoplankton cells to solar UV (Figs. 2 and 3a) gives a new perspective of the interactive effects of cell size and UV on marine primary production. The laboratory (Barbieri et al. 2002) and field (Helbling et al. 2003; Mengelt and Prézelin 2005; Gao et al. 2007a, b) studies have indicated that solar UV could drive photosynthesis of coastal phytoplankton and increase the primary productivity. Consistent with these results, the UV-utilizing ability of phytoplankton was observed here, but only in larger cells (Fig. 2). Larger cells have the ability to biosynthesize and accumulate UV-absorbing compounds (UVACs; e.g., mycosporine-like amino acids) while smaller ones have not (Raven 1991; Garcia-Pichel 1994). Apart from the protective role that the UVACs play in combating harmful UV (Raven 1991; Garcia-Pichel 1994; Sinha and Häder 2008), these compounds indicated by Gao et al. (2007a) might fill the role of an antenna to absorb and transmit UV energy to reaction center of photosystem II to drive photosynthesis, resulting in the UV-driven photosynthesis that occurred in larger but not smaller cells at PAR-free (Fig. 2) or -limiting conditions (Fig. 3a). This also explains why the UV-induced reduction of photosynthetic CO_2 fixation was lower in large-cell-dominated coastal water than small-cell-rich pelagic water (Li et al. 2011). Moreover, the higher photosynthetic rate in large-sized but not in small-sized cell assemblages (Fig. 3a) might be associated with a higher PSII photochemical efficiency characteristic of certain taxonomic groups, such as diatoms (Cermeño et al. 2005), which often dominate the study waters (Gao et al. 2007a, b; Li et al. 2009; Wu et al. 2010).

Differential responses to solar UVR by phytoplankton assemblages from Nan'ao to Xisha coastal water (Fig. 2) could mainly result from the changes of cell size in communities (Table 2). Nan'ao water is nutritious due to the local aquaculture and land-derived runoffs (Guo and Huang 2006), and thus more abundant of larger cells (Gao et al. 2007a, b; Li et al. 2009; Wu et al. 2010); while Xisha water that is located far from the mainland is oligotrophic and more plentiful of smaller cells (Li et al. 2012). High quantities of UVACs are known to occur in larger cells, but not in their smaller complements (Raven 1991; Garcia-Pichel 1994). Much higher levels of UVACs have also been observed in dinoflagellates with larger cell volume than in diatoms with small cell volume (Marcoval et al. 2007). More efficient UV-utilizing ability of phytoplankton assembly from Nan'ao than Xisha could ascertain the notion that the UVACs play a pivotal role in absorbing and transmitting UV energy to the reaction center of photosystem II, thereby driving CO_2 fixation in larger cells (Fig. 2). High nutrient level, e.g., nitrogen could increase the UVAC content in cells (Marcoval et al. 2007), that might account for the high UV-utilizing ability of phytoplankton from nutritious coastal water. This was eliminated in this study since the small cells (<5 μm) in the same nutrient-rich water (Nan'ao) did not use any UV energy for carbon fixation as compared to their larger complements (Fig. 2). Wu et al. (2010) also noticed a similar differential effect of solar UV on the primary production in the same water, due to the seasonal species transition.

Differential UV effects on phytoplankton, related to their cell size, generalize a crucial perspective in view of biological oceanography if considering the great variations (<1–10^3 μm) in phytoplankton cell size in communities over the temporal or spatial scales (Raven 1998; Li 2002; Finkel et al. 2010). Previous studies have indicated that the surface phytoplankton productivity was higher in the coastal than the pelagic water of the South China Sea even in the presence of UVR (Li et al. 2011). The size-dependent responses to solar UV and photosynthetic capability as well as the differently sized populations in different waters certainly modulate the amount of CO_2 sequestered in the oceans. In addition, since UV and PAR of different wavelengths are attenuated disproportionally downward water column, even within the upper mixing layer, photosynthetic performance and carbon fixation can differ at different depths or during a vertical mixing cycle; in return, the physiological effects of UV radiation on differently sized cells may determine their abundance in waters of different environmental conditions.

Acknowledgments This study was supported by the National Natural Science Foundation (40930846, 41120164007, and 41206132), National Basic Research Program of China (2009CB421207), Program for Changjiang Scholars and Innovative Research Team (IRT0941), China–Japan collaboration project from MOST (S2012GR0290), Special Research Fund for the National Non-profit Institutes (2008M15), and CAS Knowledge Innovation Program (SQ201115). The authors are grateful to Weizhou Chen (Nan'Ao Marine Biology Station, Shantou University) and Zhiwei Che (Sanya Marine Environment Monitoring Station, SOA) for their experimental assistance.

References

Agustí, S., and M. Llabrés. 2007. Solar radiation-induced mortality of marine pico-phytoplankton in the oligotrophic ocean. *Photochemistry and Photobiology* 83: 793–801.

Barbieri, E.S., V.E. Villafañe, and E.W. Helbling. 2002. Experimental assessment of UV effects upon temperate marine phytoplankton when exposed to variable radiation regimes. *Limnology and Oceanography* 47: 1648–1655.

Behrenfeld, M.J., and P.G. Falkowski. 1997. A consumer's guide to phytoplankton primary productivity models. *Limnology and Oceanography* 42: 1479–1491.

Buma, A.G.J., P. Boelen, and W.H. Jeffrey. 2003. UVR-induced DNA damage in aquatic organisms. In *UV Effects in Aquatic Organisms and Ecosystems*, ed. E.W. Helbling and H.E. Zagarese, 291–327. Cambridge: The Royal Society of Chemistry.

Cermeño, P., P. Estévez-Blanco, E. Marañón, and E. Fernañdez. 2005. Maximum photosynthetic efficiency of size-fractionated phytoplankton assessed by ^{14}C uptake and fast repetition rate fluorometry. *Limnology and Oceanography* 50: 1438–1446.

Chen, Y.L. 2005. Spatial and seasonal variations of nitrate-based new production and primary production in the South China Sea. *Deep Sea Research* 52: 319–340.

Davidson, A.T., H.J. Marchant, and W.K. De la Mare. 1996. Natural UV-B exposure changes the species composition of Antarctic phytoplankton in a mixed culture. *Aquatic Microbiology Ecology* 10: 299–305.

Eilers, P.H.C., and J.C.H. Peeters. 1988. A model for the relationship between light intensity and the rate of photosynthesis in phytoplankton. *Ecological Modeling* 42: 199–215.

Finkel, Z.V., J. Beardall, K.J. Flynn, A. Quigg, T.A.V. Rees, and J.A. Raven. 2010. Phytoplankton in a changing world: cell size and elemental stoichiometry. *Journal of Plankton Research* 32: 119–137.

Fujiki, T., and S. Taguchi. 2002. Variability in chlorophyll a specific absorption coeffcient in marine phytoplankton as a function of cell size and irradiance. *Journal of Plankton Research* 24: 859–874.

Gao, K., Y. Wu, G. Li, H. Wu, V.E. Villafañe, and E.W. Helbling. 2007a. Solar UV-radiation drives CO_2-fixation in marine phytoplankton: a double-edged sword. *Plant Physiology* 144: 54–59.

Gao, K., G. Li, E.W. Helbling, and V.E. Villafañe. 2007b. Variability of UVR effects on photosynthesis of summer phytoplankton assemblages from a tropical coastal area of the South China Sea. *Photochemistry and Photobiology* 83: 802–809.

Gao, K., Z. Ruan, V.E. Villafañe, J.P. Gattuso, and E.W. Helbling. 2009. Ocean acidification exacerbates the effect of UV radiation on the calcifying phytoplankter *Emiliania huxleyi*. *Limnology and Oceanography* 54: 1855–1862.

Garcia-Pichel, F. 1994. A model for internal self-shading in planktonic organisms and its implications for the usefulness of ultraviolet sunscreen. *Limnology and Oceanography* 39: 1704–1717.

Guo, Y., and C. Huang. 2006. Spatial-temporal distribution of inorganic nitrogen in the offshore water of Shantou and its related environmental factors from 2000 to 2003. *Journal of Oceanography in Taiwan Strait* 25: 194–201 (in Chinese).

Häder, D.P. 2011. Does enhanced solar UV-B radiation affect marine primary producers in their natural habitats? *Photochemistry and Photobiology* 87: 263–266.

Häder, D.P., M. Lebert, R. Marangoni, and G. Colombetti. 1998. ELDONET–European Light Dosimeter Network hardware and software. *Journal of Photochemistry and Photobiology B: Biology* 52: 51–58.

Häder, D.P., H.D. Kumar, R.C. Smith, and R.C. Worrest. 2007. Effects of solar UV radiation on aquatic ecosystems and interactions with climate change. *Photochemical and Photobiological Science* 6: 267–285.

Helbling, E.W., K. Gao, R.J. Gonçalves, H. Wu, and V.E. Villafañe. 2003. Utilization of solar UV radiation by coastal phytoplankton assemblages off SE China when exposed to fast mixing. *Marine Ecology Progress Series* 259: 59–66.

Hogue, V.E., F.P. Wilkerson, and R.C. Dugdal. 2005. Ultraviolet-B radiation effects on natural phytoplankton assemblages of central San Francisco bay. *Estuaries and Coasts* 28: 190–203.

Holm-Hansen, O., and E.W. Helbling. 1995. Técnicas para la medición de la productividad primaria en el fitoplancton. In *Manual de Métodos Ficológicos*, ed. K. Alveal, M.E. Ferrario, E.C. Oliveira, and E. Sar, 329–350. Concepción: Universidad de Concepción.

Jeffrey, W.H., P. Aas, M. Lyons, R.B. Coffin, R.J. Pledger, and D.L. Mitchell. 1996. Ambient solar radiation-induced photodamage in marine bacterioplankton. *Photochemistry and Photobiology* 64: 419–427.

Karentz, D., J.E. Cleaver, and D.L. Mitchell. 1991. Cell survival characteristics and molecular responses of Antarctic phytoplankton to ultraviolet-B radiation. *Journal of Phycology* 27: 326–341.

Laurion, I., and W.F. Vincent. 1998. Cell size versus taxonomic composition as determinants of UV-sensitivity in natural phytoplankton communities. *Limnology and Oceanography* 43: 1774–1779.

Li, W.K.W. 2002. Macroecological patterns of phytoplankton in the northwestern North Atlantic Ocean. *Nature* 419: 154–157.

Li, G., Y. Wu, and K. Gao. 2009. Effects of typhoon Kaemi on coastal phytoplankton assemblages in the South China Sea, with special reference to the effects of solar UV radiation. *Journal of Geophysical Research* 114: G04029. doi:10.1029/2008JG000896.

Li, G., K. Gao, and G. Gao. 2011. Differential impacts of solar UV radiation on photosynthetic carbon fixation from the coastal to offshore surface waters in the South China Sea. *Photochemistry and Photobiology* 87: 329–334.

Li, G., L. Huang, H. Liu, Z. Ke, Q. Lin, G. Ni, J. Yin, K. Li, X. Song, P. Shen, and Y. Tan. 2012. Latitudinal variability (6°S-20°N) of early-summer phytoplankton species composition and size-fractioned productivity from the Java Sea to the South China Sea. *Marine Biology Research* 8: 163–171.

Marcoval, M.A., V.E. Villafañe, and E.W. Helbling. 2007. Interactive effects of ultraviolet radiation and nutrient addition on growth and photosynthesis performance of four species of marine phytoplankton. *Journal of Photochemistry and Photobiology B: Biology* 89: 78–87.

Mei, Z., Z.V. Finkel, and A.J. Irwin. 2011. Phytoplankton growth allometry and size-dependent C:N stoichiometry revealed by a variable quota model. *Marine Ecology Progress Series* 434: 29–43.

Mengelt, C., and B.B. Prézelin. 2005. UVA enhancement of carbon fixation and resilience to UV inhibition in the genus *Pseudonitzschia* may provide a competitive advantage in high UV surface waters. *Marine Ecology Progress Series* 301: 81–93.

Porra, R.J. 2002. The chequered history of the development and use of simultaneous equations for the accurate determination of chlorophylls *a* and *b*. *Photosynthesis Research* 73: 149–156.

Raven, J.A. 1991. Responses of photosynthetic organisms to increased solar UV-B. *Journal of Photochemistry and Photobiology B: Biology* 9: 239–244.

Raven, J.A. 1998. Small is beautiful: the picophytoplankton. *Functional Ecology* 12: 503–513.

Raven, J.A., and J.E. Kübler. 2002. New light on the scaling of metabolic rate with the size of algae. *Journal of Phycology* 38: 11–16.

Roy, S., B. Mohovic, S.M. Gianesella, I. Schloss, M. Ferrario, and S. Demers. 2006. Effects of enhanced UV-B on pigment-based phytoplankton biomass and composition of mesocosm-enclosed natural marine communities from three latitudes. *Photochemistry and Photobiology* 82: 909–912.

Sigee, D.C. 2005. Freshwater microbiology: biodiversity and dynamic interactions of microorganisms in the freshwater environment. In *Freshwater Microbiology*, ed. D.C. Sigee, 105–180. England: Wiley.

Sinha, R.P., and D.P. Häder. 2008. UV-protectants in cyanobacteria. *Plant Science* 174: 278–289.

Villafañe, V.E., K. Sundbäck, F.L. Figueroa, and E.W. Helbling. 2003. Photosynthesis in the aquatic environment as affected by UVR. In *UV Effects in Aquatic Organisms and Ecosystems*, ed. E.W. Helbling and H.E. Zagarese, 357–397. Cambridge: The Royal Society of Chemistry.

Wu, Y., K. Gao, G. Li, and E.W. Helbling. 2010. Seasonal impacts of solar UV radiation on the photosynthesis of phytoplankton assemblages in the coastal water of the South China Sea. *Photochemistry and Photobiology* 86: 589–596.

Xu, J., and K. Gao. 2010. Use of UV-A energy for photosynthesis in the red macroalgae. *Gracilaria lemaneiformis Photochemistry and Photobiology* 86: 580–585.